ACS SYMPOSIUM SERIES 730

Spectroscopy of Superconducting Materials

Eric Faulques, EDITOR
Institut des Matériaux

American Chemical Society, Washington, DC

Chapter 15

Persistent Photoconductivity in High-T_c Superconductors

Axel Hoffmann[1], Z. F. Ren[2], J. Y. Lao[2], J. H. Wang[2], D. Girata[3], W. Lopera[4], P. Prieto[4], and Ivan K. Schuller[1]

[1]Department of Physics, University of California at San Diego, 9500 Gilman Drive, La Jolla, CA 92093–0319
[2]State University of New York at Buffalo, Buffalo, NY 14260–3000
[3]Universidad de Antioquia, Medellin, Colombia
[4]Universidad del Valle, Cali, Colombia

Persistent photoconductivity is an interesting and unusual property of high T_c superconductors. Underdoped $YBa_2Cu_3O_{6+\delta}$ shows upon illumination a decrease of resistivity and an increase of T_c. These photoinduced changes are persistent at low temperatures and relax at room temperatures. A possible model for persistent photoconductivity in these materials is that electrons of photoinduced electron-hole pairs are trapped at localized states spatially separated from the conduction layer. We recently measured persistent photoconductivity in $Tl_2Ba_2CuO_{6+\delta}$ and Y-doped $Bi_2Sr_2CaCu_{8+\delta}$, which indicates that persistent photoconductivity might be a common phenomena in high-T_c superconductors.

One of the interesting features of the high-T_c cuprates is, that their superconducting and normal state properties can be changed by varying their carrier concentration. Typically this is accomplished by chemical doping, where either one cation is substituted by another one (e.g. Sr for La in $La_{2-x}Sr_xCuO_4$), or the oxygen-stoichiometry is varied (e.g. $YBa_2Cu_3O_{6+\delta}$). Furthermore it is possible to change the carrier concentration in some of the high-T_c superconductors by illumination, and thus "photodope" these materials. This persistent photoconductivity (*1*) and persistent photoinduced superconductivity (*2*) was first observed in $RBa_2Cu_3O_{6+\delta}$ (R = rare earth or yttrium), and recently also in cuprates without CuO chains, such as $Tl_2Ba_2CuO_{6+\delta}$ (*3*) and Y-doped $Bi_2Sr_2CaCu_{8+\delta}$.

This article will be structured as follows. First we will review the persistent photoconductivity and persistent photoinduced superconductivity as it is observed in $RBa_2Cu_3O_{6+\delta}$ and discuss theoretical models for this effect. Following we will present more recent data on similar effects in chainless cuprates and discuss the implications of these results.

Due to the finite penetration depth of light (typically 1000 Å) all photoconductivity measurements were made on thin films. *C*-axis oriented RBa$_2$Cu$_3$O$_{7-\delta}$ thin films were grown using magnetron sputtering on (100) MgO and (100) SrTiO$_3$ substrates (*4*). After growth these samples were fully oxygenated ($\delta \approx 0$). In order to prepare RBa$_2$Cu$_3$O$_{6+\delta}$ thin films with a specific oxygen content ($\delta > 0$), they were annealed at 500° C following pressure-temperature curves for a specific stoichiometry of the phase diagram (*5*). After annealing the oxygen content was determined by the *c*-axis parameter (*6*) measured by high resolution X-ray diffraction and by T_c (*7*) for the superconducting films.

The resistivity measurements were done with a four probe technique, with the sample either directly immersed in liquid nitrogen, in a close cycle refrigerator, or in a He-flow cryostat, each equipped with optical quartz windows. For the illumination several different light sources were used. Most of the excitation measurements were done using a halogen lamp or an Ar laser (λ = 514 nm), with a typical power density at the sample surface of 1 Wcm^{-2}. For measuring spectral dependencies a 1000 W Hg-Xe arc lamp was used with an infrared water filter to protect the sample and the optics from excessive heating. Specific wavelengths in the range 250–900 nm were chosen with interference band-pass-filters having a bandwidth of 10 nm. Using this setup the power density of monochromatic light ranged between 0.04 and 5 mWcm^{-2}. After each light excitation the sample was relaxed at room temperature while monitoring the resistivity to determine when the sample was fully relaxed.

Basic Effect. The basic effect of illumination on the resistivity and T_c is shown in Figure 2 for an underdoped GdBa$_2$Cu$_3$O$_{6.45}$ film. Before illumination the temperature dependence of the resistivity shows a minimum and an onset of superconductivity at roughly 20 K. After white light illumination for 8 h at 95 K, the lamp is turned off and the resistance is measured again as a function of temperature. The resistance changes such that the normal state resistance is metallic, decreases substantially and the T_c increases by more than 10 K. Notice that the change in resistivity and T_c is not due to heating, since the illumination is stopped during the measurement and heating would increase the resistivity and decrease the T_c. Furthermore this photoinduced change of T_c is remarkably different from the effect of illumination on a low T_c superconductor, which causes a deterioration of the superconducting properties due to pairbreaking (*8*).

Excitation and Relaxation. These photoinduced changes in RBa$_2$Cu$_3$O$_{6+\delta}$ thin films are persistent if the sample is kept at low temperatures ($\leq$ 100 K), and relax if the sample is warmed up to room temperature. The time dependence of the excitation and of the relaxation is shown in Figure 1. For the excitation, the light source was switched on at $t = 0$, while the sample was kept at 95 K. For the relaxation, the temperature was raised from 95 to 300 K in about 12 min near $t = 0$. The time dependence of both the excitation and the relaxation follows a stretched exponential, which is given by (*9*):

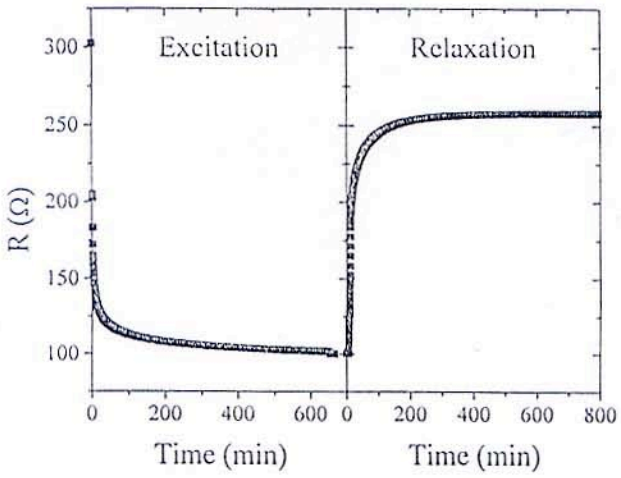

Figure 1. Time dependence of the excitation and relaxation of persistent photoconductivity in $GdBa_2Cu_3O_{6.4}$ film (Reproduced with permission from reference 10. Copyright 1995.)

$$\rho(t) = \rho(t=\infty) + \Delta\rho_{max}\exp\left[-\left(t/\tau\right)^{\beta}\right]. \quad (1)$$

Here $\Delta\rho_{max} = \rho(t=0)-\rho(t=\infty)$ is the difference between the initial and the saturation resistivity, τ is a characteristic excitation or relaxation time, and β is a dispersion parameter $0<\beta<1$. The relaxation shows a thermal activated behavior with an energy barrier of 0.9±0.1 eV (9). Besides this thermal relaxation it also possible to partially

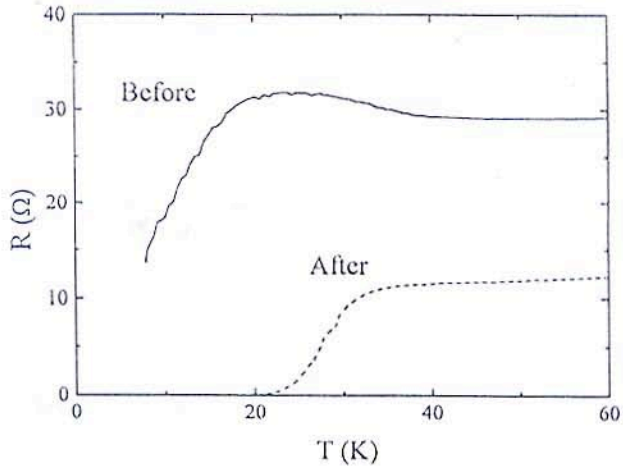

Figure 2. Temperature dependence of the resistance for a $GdBa_2Cu_3O_{6.45}$ film before (solid line) and after (dashed line) illumination (Reproduced with permission from reference 10. Copyright 1995.)

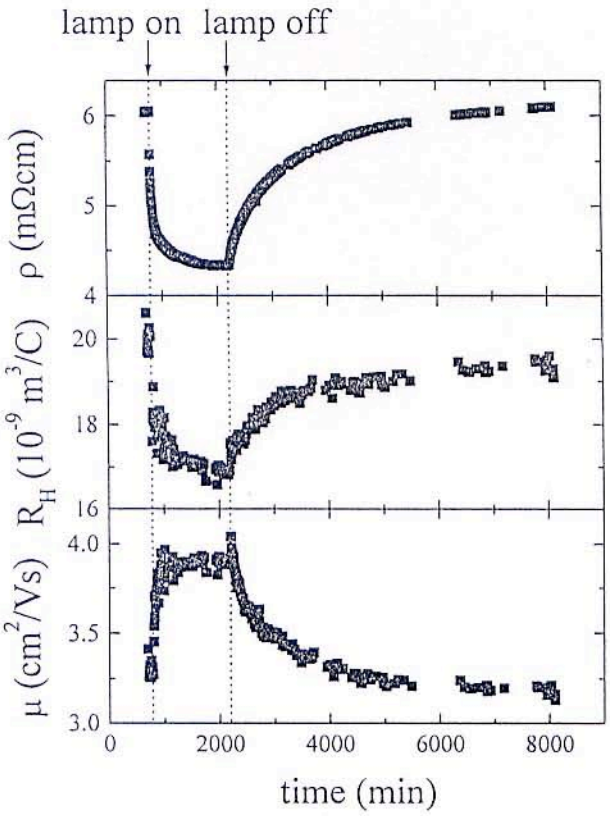

Figure 3. Time dependence of the resistivity ρ, Hall coefficient R_H, and Hall mobility $\mu = c(|R_H|/\rho)$ during excitation and relaxation in an $YBa_2Cu_3O_{6.5}$ film (Reproduced with permission from reference 12. Copyright 1992 American Physical Society.)

quench (≈ 5%) the persistent photoconductivity using infrared light (0.8–1.3 eV) (*11*).

Other Photoinduced Changes. In addition to the decrease in the resistivity there are also photoinduced changes in the Hall coefficient R_H and the Hall mobility $\mu = c(|R_H|/\rho)$ (*12*). These changes are shown in Figure 3 for an $YBa_2Cu_3O_{6.5}$ film measured at room temperature. Clearly both R_H and μ have the same time dependence during excitation and relaxation as ρ. In a simple one band model, the Hall coefficient R_H is inversely proportional to the carrier density. Thus the data in Figure 3 suggest that the carrier density increases, which results in a decrease in resistivity. In addition the Hall mobility μ changes and contributes to the variation in the resistivity ρ (*12*). These variations in the transport properties are also accompanied by a change of the *c*-axis (*13*). Upon illumination the *c*-axis contracts, which is contrary to thermal expansion due to heating. Interestingly, all the observed photoinduced effects are similar to changes due to increased oxygen doping in $RBa_2Cu_3O_{6+\delta}$ (*14*).

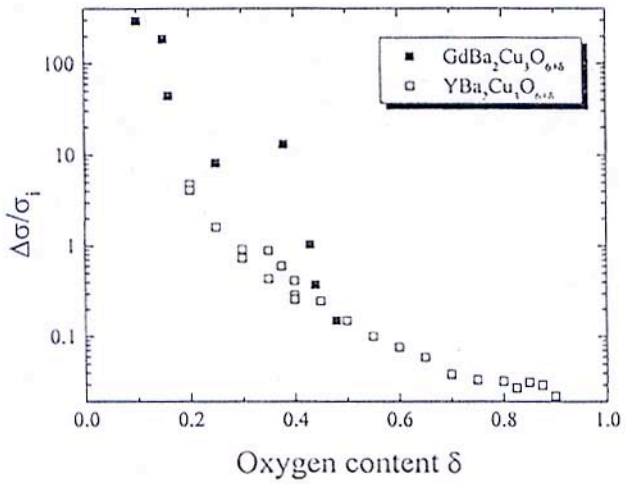

Figure 4. Relative change in conductivity $\Delta\sigma/\sigma_i$ as a function of oxygen content x of RBa$_2$Cu$_3$O$_{6+\delta}$. Solid symbols refer to GdBa$_2$Cu$_3$O$_{6+\delta}$, while open symbols refer to YBa$_2$Cu$_3$O$_{6+\delta}$ (Reproduced with permission from reference 15. Copyright 1995 American Physical Society.)

Doping Dependence. As shown above, the photoinduced effects in RBa$_2$Cu$_3$O$_{6+\delta}$ films are remarkably similar to oxygen doping effects. Also it has been shown that persistent photoconductivity only occurs in RBa$_2$Cu$_3$O$_{6+\delta}$ if there are oxygen vacancies in the CuO chains (*13*). Therefore it is interesting to take a look at the influence of oxygen stoichiometry on the persistent photoconductivity in these materials. In Figure 4 the saturation conductivity change after illumination at 95 K is shown as a function of oxygen content δ. The data is normalized to the conductivity before illumination σ_i, since the conductivity decreases strongly with decreasing oxygen content δ. From Figure 4 it is clear that the photoinduced effect is strongly enhanced for fully deoxygenated RBa$_2$Cu$_3$O$_{6+\delta}$ (*15*).

Spectral Dependence. Early measurements of the spectral dependence of persistent photoconductivity in RBa$_2$Cu$_3$O$_{6+\delta}$ showed an onset at 1.6 eV (*9*,*16*). We extended the measurement of the spectral dependence into the UV region, which is shown in Figure 5. It has been shown that for a given wavelength, the magnitude of the photoinduced effects depends only on the incident photon dose

$$n = \frac{I \times t}{\hbar\omega}, \tag{2}$$

where I is the light intensity at the sample surface; t the measurement time, and $\hbar\omega$ the photon energy. The spectral efficiency in Figure 5 is given by $1/n'$, where n' is the photon dose necessary for a 2% reduction of the resistivity. Notice that $1/n'$ is proportional to the spectral efficiency η defined by Kudinov *et al.* (*9*):

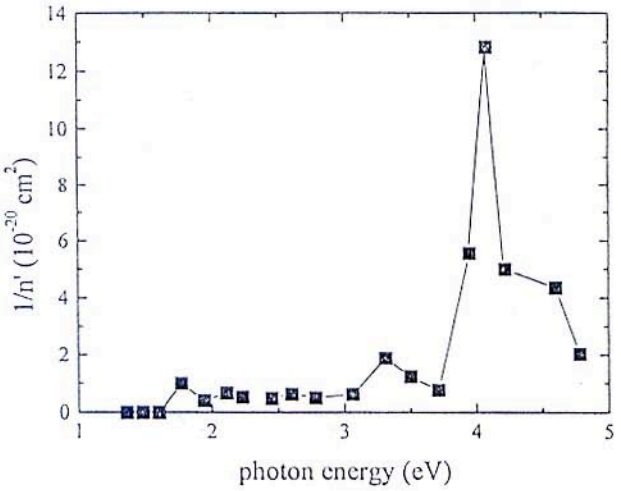

Figure 5. Spectral efficiency of the persistent photoconductivity for $GdBa_2Cu_3O_{6.3}$ (Reproduced with permission from reference 17. Copyright 1996 American Physical Society.)

$$\eta(\hbar\omega) = \frac{1}{R(0)} \left. \frac{\partial R(n)}{\partial n} \right|_{(n=0)} . \qquad (3)$$

It is worthwhile to mention, that there has been also observed an effect similar to persistent photoconductivity in $YBa_2Cu_3O_{6.0}$ upon irradiation with X-rays (*18*).

There are two features of the spectral dependence, which are remarkable. First the persistent photoconductivity shows an onset at 1.6 eV. Below 1.6 eV there is essentially no change of the resistivity upon illumination. This energy corresponds to the charge transfer gap in insulating $YBa_2Cu_3O_{6.1}$ as observed with optical absorption measurements (*19*). Interestingly this charge transfer gap vanishes in optical absorption measurements with increased doping (*19*), while it is still clearly resolved in photoconductivity measurements even for superconducting $YBa_2Cu_3O_{6+\delta}$ samples (*9*,*16*,*20*). This means that there are only localized states below 1.6 eV.

The second striking spectral feature is the peak of the spectral efficiency at 4.1 eV. This peak has been attributed to a $3d_{3z^2-1}$ to $4p_x$ electronic transition of Cu^{1+} atoms in an O-Cu-O dumbbell (*21*). These Cu^{1+} atoms are locate in the CuO chains and have an oxygen vacancy on both sides. The enhancement observed for the persistent photoconductivity at 4.1 eV is much stronger, than what can be expected from the increased absorption at this energy alone (*17*). Thus this implies that the persistent photoconductivity is strongly enhanced as soon as an electron-hole pair is created in close proximity to an oxygen vacancy, which is also consistent with the observed doping dependence.

Theoretical Models

Since the oxygen vacancies in the CuO chains of RBa$_2$Cu$_3$O$_{6+\delta}$ play an important role for the persistent photoconductivity (*13,15,17*), there were several models developed involving specifically the CuO chains in this material. The two main models are based on either photoassisted oxygen ordering (*22*) or trapping of photogeneration of mobile carriers (*9,15*).

Photoassisted Oxygen Ordering. It has been shown, that RBa$_2$Cu$_3$O$_{6+\delta}$ samples rapidly quenched from higher temperatures show transport and structural changes during room temperature annealing similar to persistent photoconductivity (*23*). This effect of room temperature annealing was explained by oxygen ordering in the CuO chains. Furthermore, the activation energy for the relaxation of the photoinduced effects is with 0.9±0.1 eV (*9*) close to the oxygen diffusion activation energy of 1.3 eV (*24*). This suggest that the pohotoinduced effects could be due to photoassisted oxygen ordering (*22*).

There is an important difference between oxygen ordering in quenched samples and the photoinduced effects. While in quenched samples the oxygen in the CuO chains order during room temperature annealing, the oxygen has to disorder from a metastable ordered state in the photoexcited samples during room temperature relaxation. It has been shown, that the photoexcitation process is indeed independent from oxygen disorder induced by quenching (*25*). Furthermore, the oxygen ordering model implies, that persistent photoconductivity should vanish for completely deoxygenated ($\delta \approx 0$) RBa$_2$Cu$_3$O$_{6+\delta}$ samples, contrary to the observed doping dependence (*15*). Therefore it is doubtful that the photoassisted oxygen ordering explains the persistent photoconductivity in RBa$_2$Cu$_3$O$_{6+\delta}$.

Electron Trapping. In another model the incoming photons create electron-hole pairs (*9,15*). Subsequently, the electron is trapped at an oxygen vacancy in the CuO chain, while the hole is transferred to an extended state in the CuO_2 planes and thus enhances the conductivity. This model is consistent with all the observed data so far, in particular it can explain the doping dependence (*15*) and the spectral dependence (*17*) of the persistent photoconductivity. Furthermore this mechanism is also supported by measurements of the photoluminescence in YBa$_2$Cu$_3$O$_{6.4}$ (*26*).

The photoinduced structural changes (*13*) can be understood by a lattice distortion caused by the trapped electrons. This lattice distortion gives rise to an energy barrier, which inhibits the recombination of the trapped electrons with a hole (*15*). However, it is not presently clear how the proposed models can explain the photoinduced changes in the mobility (*12*). One possibility is that the photoinduced structural modification causes the change in the mobility.

Cuprates Without CuO Chains

The above shown measurements were all done on RBa$_2$Cu$_3$O$_{6+\delta}$. One specific feature of this material that sets it apart from most other high T_c cuprates is that its structure contains CuO chains. Since early measurements did not show persistent photocon-

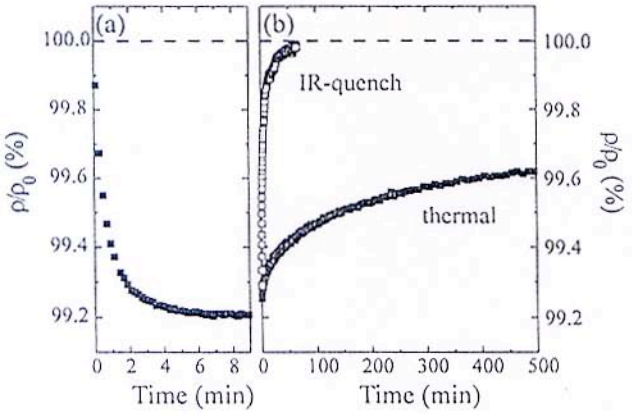

Figure 6. Excitation (a) and relaxation (b) of the persistent photoconductivity in $Tl_2Ba_2CuO_{6+\delta}$. In (b) solid symbol refer to thermal relaxation and open symbols refer to infrared quenching at 1100 nm. ρ_0 is the initial resistivity of the fully relaxed sample, which is also indicated by dashed lines (Reproduced with permission from reference 3. Copyright 1997 American Physical Society.)

ductivity in other cuprates besides $RBa_2Cu_3O_{6+\delta}$ (*22*), the theoretical models involved in one way or another specifically these CuO chains. We will now show measurements of persistent photoconductivity in cuprates *without* CuO chains (*3*). Thus, clearly persistent photoconductivity does not require the presence of CuO chains and might be a more common effect in these materials.

$Tl_2Ba_2CuO_{6+\delta}$. In contrast to $RBa_2Cu_3O_{6+\delta}$, $Tl_2Ba_2CuO_{6+\delta}$ has a rather simple structure with only one CuO_2 plane per unit cell sandwiched between TlO layers, and *no* CuO chains. By increasing in $Tl_2Ba_2CuO_{6+\delta}$ the oxygen concentration δ, it is possible to decrease the T_c from 85–0 K (*27*). Thus the $T_2Ba_2CuO_{6+\delta}$ films used for the persistent photoconductivity measurements are in the *overdoped* regime, meaning a decreasing T_c with increasing carrier density n ($\partial T_c / \partial n < 0$), while the $RBa_2Cu_3O_{6+\delta}$ films are in the *underdoped* regime ($\partial T_c / \partial n > 0$).

The $Tl_2Ba_2CuO_{6+\delta}$ films were grown by RF sputtering on $SrTiO_3$ substrates (*28-31*). The thicknesses of the films were 500–800 Å, so that the films were transparent and completely penetrated by the light used in the experiments. After growth, the T_c of the films was adjusted between 10 and 80 K by annealing in argon or air. The persistent photoconductivity measurements were performed in the same setup as for the $RBa_2Cu_3O_{6+\delta}$ films.

Basic Effect. The basic effect of illumination on the resistivity of $Tl_2Ba_2CuO_{6+\delta}$ is shown in Figure 7. Depending on the doping and the wavelength the normal state resistivity ρ and the T_c can either increase or decrease. The $Tl_2Ba_2CuO_{6+\delta}$ thin film with an initial T_c of 60 K (see Figure 7(a)) shows an increase in both T_c and ρ during illumination with 1000 nm light, while both T_c an ρ decrease during illumination with 400 nm light. In contrast, a higher doped $Tl_2Ba_2CuO_{6+\delta}$ with a T_c of 13 K,

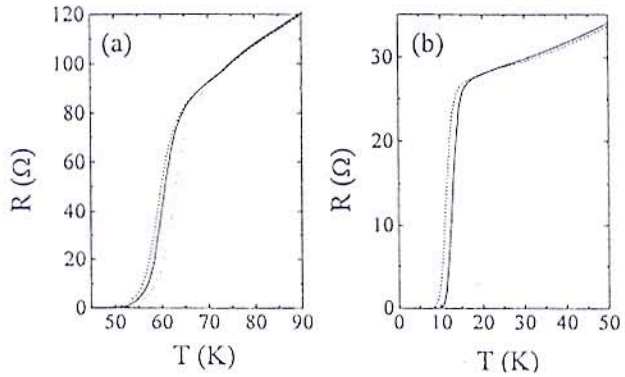

Figure 7. Resistance vs. temperature during (dashed or dotted line) and without (solid line) illumination for $Tl_2Ba_2CuO_{6+\delta}$ thin films with different doping. (a) Initial $R(T)$ (solid line) with T_c = 670 K and $R(T)$ during illumination with 1000 nm (dashed-dotted line) and 400 nm (dashed line) light. (b) Initial $R(T)$ with T_c = 13 K (solid line) and $R(T)$ during illumination with 440 nm (dashed line) light (Reproduced with permission from reference 3. Copyright 1997 American Physical Society.)

shows only a decrease of T_c and ρ, which is shown in Figure 7(b) for 440 nm light. Notice, that unlike in $R Ba_2Cu_3O_{6+\delta}$, the change of T_c and ρ have always the same sign, which is due to the $Tl_2Ba_2CuO_{6+\delta}$ being overdoped. Also the photoinduced changes in T_c and ρ are smaller than the ones in underdoped $R Ba_2Cu_3O_{6+\delta}$, but comparable to almost optimally doped $R Ba_2Cu_3O_{6+\delta}$ (*15*, see also Figure 4).

One important difference between the measurements on $Tl_2Ba_2CuO_{6+\delta}$ (Figure 7) and $R Ba_2Cu_3O_{6+\delta}$ (Figure 2) is the temperature dependence of the resistivity for $Tl_2Ba_2CuO_{6+\delta}$ was measured *during* illumination instead of with the light turned off. The reason for this is that in $Tl_2Ba_2CuO_{6+\delta}$ the persistent photoconductivity slowly relaxes even at low temperatures. However, any significant thermal heating due to the illumination can be ruled out, because of the very low power densities (≈ 0.1 $mWcm^{-2}$) used during the measurements.

The time dependence of the excitation and the relaxation is shown in Figure 6 for the $Tl_2Ba_2CuO_{6+\delta}$ sample with a T_c of 13 K measured at 30 K. Obviously the time constant for the excitation is much faster than for $R Ba_2Cu_3O_{6+\delta}$ (see Figure 1), and also there is still some thermal relaxation to the initial ρ even at 30 K, in contrast to $R Ba_2Cu_3O_{6+\delta}$ where there is essentially no thermal relaxation at temperatures below approximately 100 K (*9*). This thermal relaxation in $Tl_2Ba_2CuO_{6+\delta}$ becomes faster at higher temperatures and takes only a few minutes above 100 K. Again both the excitation and the relaxation shows a stretched exponential behavior (see equation 1).

Also it is possible in the higher doped sample to quench the resistivity back to its initial value by illuminating the sample with 1100 nm light [see Figure 6(b)]. The original resistivity is this way recovered within one hour, unlike in $R Ba_2Cu_3O_{6+\delta}$ where so far only a partial quenching of the persistent photoconductivity has been observed (*11*).

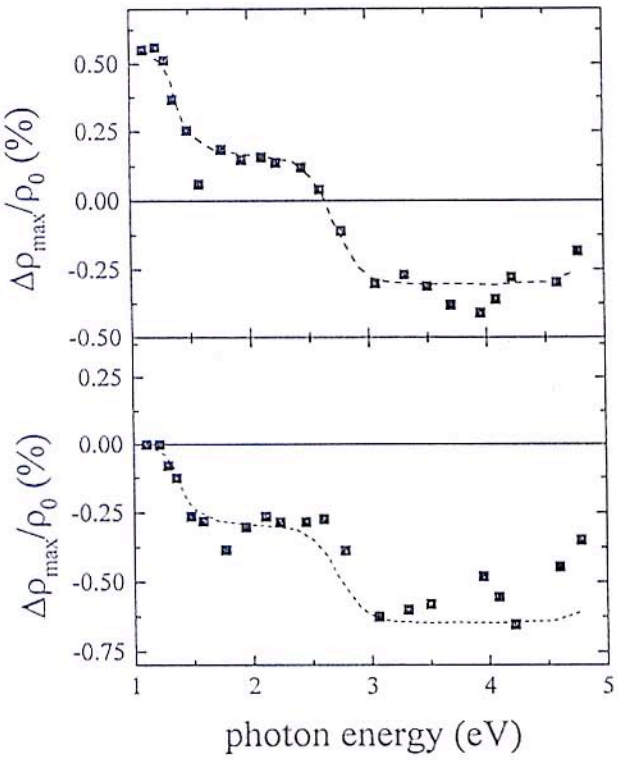

Figure 8. Spectral dependence of persistent photoconductivity in $Tl_2Ba_2CuO_{6+\delta}$ for the T_c = 60 K (a) and the T_c 13 K (b) sample. The dashed lines are guides to the eye (Reproduced with permission from reference 3. Copyright 1997 American Physical Society.)

Spectral Dependence. The spectral dependence of the photoinduced resistivity changes at saturation $\Delta\rho_{max}$ normalized to the initial resistivity ρ_0 are shown in Figure 8, as they were measured at (a) 85 K and (b) 30 K for the T_c = 60 K and 13 K sample, respectively. Independent of doping there are three distinct energy regions, below 1.3 eV, 1.3–2.8 eV, and above 2.8 eV. In each of these energy regions $\Delta\rho_{max}$ is almost constant. For the lower doped $Tl_2Ba_2CuO_{6+\delta}$ sample (T_c = 60 K), the energy region with a photoinduced increase of ρ changes continuously into the region with a photoinduced decrease of ρ. On the other hand, the spectral efficiency $\eta(\hbar\omega)$ (see equation 3) is featureless from 1–4.8 eV. Interestingly, the onset of persistent photoconductivity for the higher doped $Tl_2Ba_2CuO_{6+\delta}$ (T_c = 13 K) sample is observed at a similar energy (1.3 eV) as it is for the underdoped $RBa_2Cu_3O_{6+\delta}$ (onset at 1.6 eV, see Figure 5).

This spectral dependence, with two plateaus, can be explained if one uses a similar purely electronic mechanism, as the one proposed for $RBa_2Cu_3O_{6+\delta}$ (*1*,*3*,*15*). This model proposes that in $RBa_2Cu_3O_{6+\delta}$ oxygen vacancies in the CuO chains trap photogenerated electrons. In $Tl_2Ba_2CuO_{6+\delta}$ there are two types of structural defects

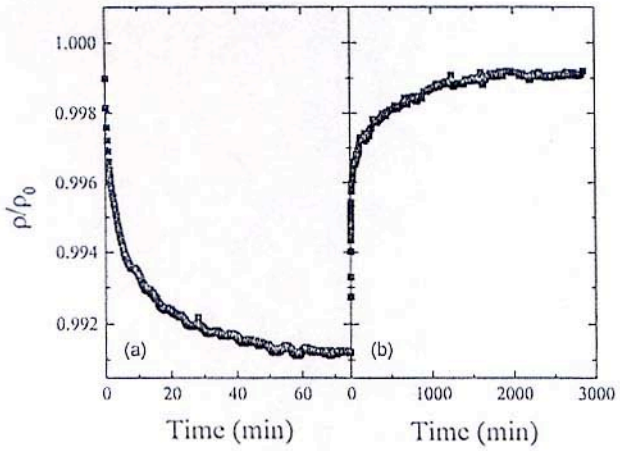

Figure 9. Time dependence of persistent photoconductivity in $Bi_2Sr_2Ca_{1-x}Y_xCu_{8+\delta}$ during (a) excitation and (b) relaxation. (Reproduced with permission from reference 3. Copyright 1997 American Physical Society.)

(*32*), Cu for Tl substitution in the TlO layers and interstitial oxygen between the TlO layers, which might trap the photogenerated electrons. The presence of these two types of defects can explain the observed spectral dependence with two excited levels (see Figure 8). If this model is correct, then persistent photoconductivity should be present in most high-T_c cuprates, since all that it requires are localized electron states spatially separated from extended hole states in the conduction layers (CuO_2 planes).

On the other hand it is unlikely that the oxygen ordering model proposed for $RBa_2Cu_3O_{6+\delta}$ (*22*) can explain the observed persistent photoconductivity in $Tl_2Ba_2CuO_{6+\delta}$. It has been shown that structural ordering in $Tl_2Ba_2CuO_{6+\delta}$ always leads *only* to a decrease in resistivity and thus is clearly irreversible unless thermally relaxed (*33*). In contrast, the sign of the photoinduced resistivity changes depends on doping (see Figures 6 and 8) and is reversible (see Figure 6). In order for the structural ordering mechanism to be correct, this would imply the unlikely case that illumination with a single wavelength either *orders* or *disorders* oxygen, depending on doping or initial resistivity.

Y-doped $Bi_2Sr_2CaCu_2O_{8+\delta}$. As mentioned above the mechanism based on defect trapping of photogenerated electrons suggests that persistent photoconductivity should be a more general observed phenomenon in high-T_c cuprates. We also recently observed this effect in Y-doped $Bi_2Sr_2CaCu_2O_{8+\delta}$. These $Bi_2Sr_2Ca_{1-x}Y_xCu_2O_{8+\delta}$ samples showed an insulating temperature dependence of the resistivity. The time dependence of the photoexcitation and thermal relaxation measured at 90 K is shown in Figure 9 and follows again a stretched exponential as in equation 1. For the photoexcitation we choose a wavelength of 470 nm, since this coincides with the resonance energy 2.6 eV observed in resonant Raman scattering (*34*).

This persistent photoconductivity in Y-doped $Bi_2Sr_2CaCu_2O_{8+\delta}$ is remarkably different from the photoinduced effects in pure $Bi_2Sr_2CaCu_2O_{8+\delta}$. In pure

$Bi_2Sr_2CaCu_2O_{8+\delta}$ there is upon illumination an *irreversible increase* of the resistivity (*35*), while in the Y-doped $Bi_2Sr_2CaCu_2O_{8+\delta}$ there is a *reversible decrease* of the resistivity. It is important to notice that the *irreversible increase* of resistivity was observed in oxygen annealed overdoped $Bi_2Sr_2CaCu_2O_{8+\delta}$, and that the irreversible increase is consistent with a simple loss of oxygen during illumination. Thus these irreversible changes are probably unrelated to the persistent photoconductivity observed in the other high-T_c cuprates. So far there have no reversible changes been observed in pure $Bi_2Sr_2CaCu_2O_{8+\delta}$.

The electron trapping mechanism used to explain the persistent photoconductivity in $RBa_2Cu_3O_{6+\delta}$ and $Tl_2Ba_2CuO_{6+\delta}$ can also be used for $Bi_2Sr_2Ca_{1-x}Y_xCu_2O_{8+\delta}$. The substitution of Y for Ca might introduce localized defect states, which like in the other materials may trap photogenerated electrons. If this is the case then the persistent photoconductivity in $Bi_2Sr_2Ca_{1-x}Y_xCu_2O_{8+\delta}$ should show a similar dependence with the Y content x as the doping dependence observed for $RBa_2Cu_3O_{6+\delta}$ (see Figure 4). This may also explain the absence of any reversible photoinduced changes in pure $Bi_2Sr_2CaCu_2O_{8+\delta}$.

Other Cuprates. Besides the cuprates discussed above ($RBa_2Cu_3O_{6+\delta}$, $Tl_2Ba_2CuO_{6+\delta}$, and $Bi_2Sr_2Ca_{1-x}Y_xCu_2O_{8+\delta}$) there is to our knowledge no observation of persistent photoconductivity in other systems. But the recent results on cuprates without CuO chains suggest, that this effect is more widespread in this class of materials, as expected for the electron trapping mechanism. Indeed, we have preliminary results which suggest that persistent photoconductivity can also be observed in $La_{2-x}Sr_xCuO_4$. Furthermore, $Tl_2Ba_2CaCu_2O_8$ exhibits metastable photoinduced changes of its magnetic properties, which may be related to persistent photoconductivity (*36*).

These results may have important consequences for measurements using optical probes, e.g., Raman scattering or photoemission spectroscopy. The increased doping level during illumination, which leads to a reduced T_c, might have to be taken into account for the interpretation of the data. On the other hand the persistent photoconductivity can also be used as a tool to investigate doping effects. The reversible photodoping allows to measure in *one* sample the dependence of other physical properties on the carrier concentration in the high-T_c cuprates. Furthermore, persistent photoconductivity might exist in similar complex materials besides the high-T_c cuprates and allow to study doping dependencies, e.g. in the colossal magnetoresistive manganites, where one could expect a photoinduced transition from an insulating antiferromagnetic to a metallic ferromagnetic state (*37*).

Conclusion

In summary, we have shown persistent photoconductivity in a variety of different high-T_c cuprates ($RBa_2Cu_3O_{6+\delta}$, $Tl_2Ba_2CuO_{6+\delta}$, and $Bi_2Sr_2Ca_{1-x}Y_xCu_2O_{8+\delta}$). The effect is characterized by a reversible change of the carrier concentration upon illumination. This photoinduced change of the carrier concentration is persistent with a long lifetime at low temperatures and relaxes thermally at elevated temperatures. The photoinduced changes in turn modify the resistivity (in most cases a decrease with illumination) and the T_c (increase or decrease depending on initial doping level). The observation of

persistent photoconductivity in $Tl_2Ba_2CuO_{6+\delta}$ and $Bi_2Sr_2Ca_{1-x}Y_xCu_2O_{8+\delta}$ shows that this effect is not limited to cuprates with CuO chains.

The doping dependence in $RBa_2Cu_3O_{6+\delta}$ and the spectral dependence in $RBa_2Cu_3O_{6+\delta}$ and $Tl_2Ba_2CuO_{6+\delta}$ suggest that the persistent photoconductivity is due to an electron trapping mechanism. In this model the electron of a photogenerated electron hole pair is trapped at a localized state in the charge reservoir layer, while the remaining hole gets transferred to the conduction (CuO_2) layer. This model is in principle applicable to other cuprates as well, so that persistent photoconductivity might be a more common phenomenon in high-T_c materials.

The observed persistent photodoping effects might be important for measurements using optical probes. Furthermore these effects can also be used to study the doping dependence of other physical properties.

Acknowledgments

We gratefully acknowledge valuable discussions with D. Basov, G. Blumberg, Y. Bruynseraede, T. Endo, A. Gilabert, G. Güntherodt, J. Hasen, D. Lederman, P. Lemmens, J. Martin, D. Reznik, J. Santamaria, P. Seidel, M. Veléz, and J. Vicent. This work was supported by the NSF. Work at SUNY at Buffalo was sponsored by the New York State Energy Research and Development Authority (NYSERDA), and work at Universidad del Valle was sponsored by COLCIENCIAS. Prof. P. Prieto thanks the Guggenheim foundation for support of a sabbatical year at UCSD.

References

1. Kudinov, V. I.; Kirilyuk, A. I.; Kreines, N. M.; Laiho, R.; Lähderanta, E. *Phys. Lett. A* **1990**, *151*, 358.
2. Nieva, G.; Osquiguil, E.; Guimpel, J.; Maenhoudt, M.; Wuyts, B.; Bruynseraede, Y.; Maple, M. B.; Schuller, I. K. *Appl. Phys. Lett.* **1992**, *60*, 2159.
3. Hoffmann, A.; Schuller, I. K.; Ren, Z. F.; Lao, J. Y.; Wang, J. H. *Phys. Rev. B* **1997**, *56*, 13742.
4. Nakamura, O.; Fullerton, E. E.; Guimpel, J.; Schuller, I. K. *Appl. Phys. Lett.* **1992**, *60*, 120.
5. Osquiguil, E.; Maenhoudt, M.; Wuyts, B.; Bruynseraede, Y. *Appl. Phys. Lett.* **1992**, *60*, 1627.
6. Cava, R. J.; Batlogg, B.; Rabe, K. M.; Rietman, E. A.; Gallagher, P. K.; Rupp, L. W. *Physica C* **1988**, *156*, 523.
7. Tranquada, J. M.; Moudden, A. H.; Goldman, A. I.; Zolliker, P.; Cox, E. E.; Shirane, G.; Sinha, S. K.; Vakin, D.; Johnson, D. C.; Alvarez, M. S.; Jacobson, A. J.; Lewandowski, J. T.; Newsam, J. M. *Phys. Rev. B* **1988**, *38*, 2477.
8. *Nonequilibrium Superconductivity, Phonons, and Kapitza Boundaries*; Kenneth, E. G., Eds.; NATO Advanced Study Institute Series B: Physics; Plenum Press: New York, NY, 1981; Vol. 65.
9. Kudinov, V. I.; Chaplygin, I. L.; Kirilyuk, A. I.; Kreines, N. M.; Laiho, R.; Lähderanta, E.; Ayache, C. *Phys. Rev. B* **1993**, *47*, 9017.
10. Hasen, J. *Ph.D. Thesis*, University of California, San Diego, 1995.
11. Chew, D. C.; Federici, J. F.; Guitierrez-Solana, J.; Molina, G.; Savin, W.; Wilber, W. *Appl. Phys. Lett.* **1996**, *69*, 3260.
12. Nieva, G.; Osquiguil, E.; Guimpel, J.; Maenhoudt, M.; Wuyts, B.; Bruynseraede, Y.; Maple, M. B.; Schuller, I. K. *Phys. Rev. B* **1992**, *46*, 14249.

13. Lederman, D.; Moran, T. J.; Hasen, J.; Schuller, I. K. *Appl. Phys. Lett.* **1993**, *63*, 1276.
14. For a review, see: Markert, J. T.; Dunlap, B. D.; Maple, M. B. *MRS Bull. XIV* **1989**, *1*, 37.
15. Hasen, J.; Lederman, D.; Schuller, I. K.; Kudinov, V.; Maenhoudt, M.; Bruynseraede, Y. *Phys. Rev. B* **1995**, *51*, 1342.
16. Bud'ko, S. L.; Feng, H. H.; Davis, M. F.; Wolfe, J. C.; Hor, P. H. *Phys. Rev. B* **1993**, *48*, 16707.
17. Endo, T.; Hoffmann, A.; Santamaria, J.; Schuller, I. K. *Phys. Rev. B* **1996**, *54*, 3750.
18. Jiménez de Castro, M.; Alvarez Rivas, J. L. *Phys. Rev. B* **1996**, *53*, 8614.
19. Cooper, S. L.; Kotz, A. L.; Karlow, M. A.; Klein, M. V.; Lee, W. C.; Giapintzakis, J.; Ginsberg, D. M. *Phys. Rev. B* **1992**, *45*, 2549.
20. Markowitsch, W.; Stockinger, C.; Lang, W.; Kula, W.; Sobolewski, R. *Proceedings of the SPIE* **1996**, *2696*, 617.
21. Kelly, M. K.; Barboux, P.; Tarascon, J.-M.; Aspnes, D. E.; Bonner, W. A.; Morris, P. A. *Phys. Rev. B* **1988**, *38*, 870.
22. Osquiguil, E.; Maenhoudt, M.; Wuyts, B.; Bruynseraede, Y.; Lederman, D.; Schuller, I. K. *Phys. Rev. B* **1994**, *49*, 3675.
23. Veal, B. W.; You, H.; Paulikas, A. P.; Shi, H.; Fang, Y.; Downey, J. W. *Phys. Rev. B* **1990**, *42*, 4770.
24. Tolpygo, S. K.; Lin, J.-Y.; Gurvitch, M.; Hou, S. Y.; Phillips, J. M.; *Phys. Rev. B* **1996**, *53*, 12462.
25. Guimpel, J.; Maiorov, B.; Osquiguil, E.; Nieva, G.; Pardo, F. *Phys. Rev. B* **1997**, *56*, 3552.
26. Federici, J. F.; Chew, D.; Welker, B.; Savin, W.; Guitierrez-Solana, J.; Fink, T.; Wilber, W. *Phys. Rev. B* **1995**, *52*, 15592.
27. Kubo, Y.; Shimakawa, Y.; Manako, T.; Igarashi, H. *Phys. Rev. B* **1991**, *43*, 7875.
28. Wang, C. A.; Ren, Z. F.; Wang, J. H.; Petrov, D. K.; Naughton, M. J.; Yu, W. Y.; Petrou, A. *Physica C* **1996**, *262*, 98.
29. Ren, Z. F.; Wang, C. A.; Wang, J. H. In *Proceedings of the 10th Anniversary HTS Workshop on Physics, Materials & Applications;* Batlogg, B.; Chu, C. W.; Chu, W. K.; Gubser, D. U.; Muller, K. A., Ed.; World Scientific: Singapore, 1996; pp 199-200.
30. Ren, Z. F.; Wang, J. H.; Miller, D. J. *Appl. Phys. Lett.* **1996**, *69*, 1798.
31. Ren, Z. F.; Wang, J. H.; Miller, D. J. *Appl. Phys. Lett.* **1997**, *71*, 1706.
32. Wagner, J. L.; Chmaissem, O.; Radaelli, P. G.; Hunter, B. A.; Jorgensen, J. D.; Hinks, D. G.; Jensen, W. R. *Physics C* **1997**, *277*, 170.
33. Schilling, J. S.; Klehe, A.-H.; Looney, C; Takahashi, H.; Môri, N.; Shimakawa, Y.; Kubo, Y.; Manako, T.; Doyle, S.; Hermann, A. M. *Physica C* **1996**, *257*, 105.
34. Boekholt, M.; Moshalkov, V. V.; Güntherodt, G. *Physica C* **1992**, *192*, 191.
35. Tanabe, K.; Karimoto, S.; Kubo, S.; Tsuru, K.; Suzuki, M. *Phys. Rev. B* **1995**, *52*, 13152.
36. Szymczak, H.; Baran, M.; Gnatchanko, S. L.; Szymczak, R.; Chen, Y. F.; Ivanov, Z. G.; Johansson, L.-G. *Europhys. Lett.* **1996**, *35*, 452.
37. Kiryukhin, V.; Casa, D.; Hill, J. P.; Keimer, B.; Vigliante, A.; Tomioka, Y.; Tokura, Y. *Nature* **1997**, *386*, 813.